

# XPS investigation on the surface chemistry of corrosion products on ZnMgAl-coated steel

J. Duchoslav · M. Arndt · T. Keppert · G. Luckeneder · D. Stifter

Received: 22 January 2013 / Revised: 21 May 2013 / Accepted: 28 May 2013 / Published online: 6 July 2013  
© Springer-Verlag Berlin Heidelberg 2013

**Abstract** In this work, a novel evaluation strategy for the X-ray photoelectron spectroscopy (XPS) chemical assessment is proposed to identify the corrosion products formed on the surface of hot-dip galvanized ZnMgAl coatings after exposure to standardized salt spray tests. The experiments demonstrate that the investigated system exhibits a problematic differential charging behavior between the different compounds, an effect which cannot be fully compensated for by the flood gun of the XPS system, making a reliable evaluation of the individual spectra impossible by using standard evaluation and fitting methods. For that reason, a new effective approach—taking the different charge shifts into account—was implemented and its reliability experimentally verified on model mixtures of assumed corrosion products with known composition. With this new approach, the chemical surface composition of an industrial sample of a corroded ZnMgAl coating was revealed and discussed in order to clearly demonstrate the potential of the proposed method for future corrosion studies.

**Keywords** X-ray photoelectron spectroscopy · Surface analysis · Data fitting · Charge shift · ZnMgAl coatings · Corrosion products

## Introduction

Hot-dip galvanizing of steel sheets with zinc is well established to be a cost-effective surface treatment, providing sufficient corrosion protection. In the last decades, considerable research efforts were dedicated to improving the corrosion resistance of zinc coatings by the addition of various alloying elements, like magnesium and aluminum [1–5], with the exact anticorrosion mechanism of alloyed zinc–magnesium–aluminum coating being studied [6–8], but not yet fully understood. Since the corrosion attack mostly starts from the surface of the materials, sophisticated surface analytic methods such as X-ray photoelectron spectroscopy (XPS) play an important role in a majority of recent corrosion studies as a complementary method to other chemical, electrochemical, or physical analysis. XPS might also act as a valuable tool for studying the initial stages of corrosion, especially since the layer of formed corrosion products may be too thin for bulk sensitive methods such as for X-ray diffraction. To evaluate the acquired XPS data and determine the exact chemistry of the corrosion products formed on the surfaces of Zn-based anticorrosion coatings, many different approaches have then been used and were reported in the literature. As an example, Zhang et al. [9] studied the effect of small additions of Mn onto the corrosion behavior of Zn coatings. The presented XPS data were evaluated by using a qualitative approach: the measured peaks were de-convoluted with symmetric peaks and the binding energies of the fitted peaks were then assigned to certain chemical components

Published in the topical collection *Applied Surface Analysis* with guest editors Karl-Heinz Müller, Hubert Paulus, and Mark Schülke.

**Electronic supplementary material** The online version of this article (doi:10.1007/s00216-013-7099-3) contains supplementary material, which is available to authorized users.

J. Duchoslav (✉) · M. Arndt · D. Stifter  
Christian Doppler Laboratory for Microscopic and Spectroscopic  
Material Characterization, Center for Surface and Nanoanalysis,  
Johannes Kepler University Linz, Altenbergerstraße 69,  
4040 Linz, Austria  
e-mail: jiri.duchoslav@jku.at

T. Keppert · G. Luckeneder  
voestalpine Stahl GmbH, Voestalpine-Straße 3,  
4031 Linz, Austria

by using external sources and databases from the literature. In detail, some disproportions in the stoichiometry can be found between claimed chemical states of zinc shown simultaneously in the zinc and oxygen scans. Such imperfections may correspond to the facts concluded by Biesinger [10]: although established databases for binding energies [11, 12] or other sources of information as papers, generally provide sufficient data for chemical assessment of rather simple systems, curve-fitting data for more complicated complex systems of, e.g., mixed metal/oxides are not included in the databases, which might cause small errors or even misleading results of fitting due to a number of effects as asymmetries of peaks, multiplet, shake-up, or plasmon loss contributions. Since layers of corrosion products formed on ZnMgAl coatings may also include a large number of different, mixed chemical states of zinc, magnesium, and aluminum [6, 7]—some which may not have been fully identified and described yet—the analysis should reflect on the chemical quantification, too. The measured stoichiometry of found chemical compounds should meet the theoretical one in order to confirm the reasonableness of the analysis. Such an approach has been used by Hosking et al. [13] for a corrosion study of ZnMg-coated steel. The binding energies of symmetrically fitted peaks were compared with internal and external reference data and the revealed chemical components were simultaneously discussed with respect to their expected stoichiometry.

In this work, we present a different approach for determining the surface chemistry of corrosion products formed on the surface of hot-dip galvanized ZnMgAl-alloyed coatings. Such coatings are also routinely exposed to standardized corrosion conditions, like in salt spray tests to foster the understanding of the exact corrosion mechanisms. In this context, it is of interest to find and verify a fast and reasonable strategy for the evaluation of the XPS data in respect to the complicated and complex system of the formed corrosion products. A former fitting strategy, in analogy to that used in ref. [14] for ZnCr coatings which is based on the reconstruction of the investigated spectra by a linear combination of fitted spectra of pure reference materials, was now found to be non-functional for ZnMgAl layers giving inconsistent information on the observed stoichiometry. For that reason, a new enhanced strategy was developed, taking differential shifts of the different constituents in the composed spectra into account. This approach was successfully verified on model mixtures of reference materials of expected corrosion products. Furthermore, the procedure was finally applied for the evaluation of a rough surface of a ZnMgAl steel sheet corroded in a salt spray test, in order to reveal its surface chemistry.

## Experimental

### Reference materials

To enhance the accuracy of the curve-fitting and reasonableness of the chemical assessment, spectra of pure reference compounds were used for fitting and evaluation of the experimental XPS spectra. An already developed reference spectra library for our XPS tool, containing, e.g., Zn, ZnO,  $\text{Zn}_3(\text{PO}_4)_2$ ,  $\text{ZnCO}_3$ ,  $\text{ZnSO}_4 \cdot 7\text{H}_2\text{O}$ ,  $\text{ZnSO}_4$ , Al,  $\text{Al}_2\text{O}_3$ ,  $\text{Al}(\text{OH})_3$ , Mg, MgO,  $4\text{Mg}(\text{CO}_3) \cdot \text{Mg}(\text{OH})_2$ , was extended with known corrosion products of Zn, Mg, and Al as, e.g., stated in [6, 7]:  $\text{Zn}_5(\text{CO}_3)_2(\text{OH})_6$  (hydrozincite, basic zinc carbonate),  $\text{Zn}_5(\text{OH})_8\text{Cl}_2 \cdot \text{H}_2\text{O}$  (simonkolleite), and  $\text{Mg}_6\text{Al}_2(\text{OH})_{16}\text{CO}_3 \cdot x\text{H}_2\text{O}$  (hydrotalcite). Hydrozincite (basic zinc carbonate) was bought from Sigma Aldrich, simonkolleite and hydrotalcite were synthesized by us according to refs. [15, 16]. Raw data of XPS spectra of three main compounds of ZnO, hydrozincite, and simonkolleite can be found in the Electronic Supplementary Material (Tables S1–S3) to this article.

### Model mixtures of reference materials

For the verification of the chosen fitting method, model mixtures of reference materials were made and measured with XPS. Mixed samples of, e.g., hydrozincite–ZnO and hydrozincite–simonkolleite were prepared by mild dry milling of powders with a pestle in a mortar. The composition of the mixed samples were 50:50 wt%. To avoid any possible and undesirable reaction or a chemical change, which might have been induced by the pressure, temperature etc., the mixtures were homogenized for only a short time of 10 min. The mixtures were not characterized in terms of particle size distribution and homogeneity of mixed powders. Therefore, a direct comparison of the obtained concentrations from the top 5–7-nm surface layer region with the nominal bulk concentration is not feasible, since, e.g., smaller grains of one component could be surrounded by bigger ones of the other component, resulting in a minor percentage of the surface coverage, a fact which was also confirmed by additional scanning electron microscopy imaging. Prior to XPS analysis, the powder materials were pressed into small sheets of an indium foil. No indium could be detected in the XPS survey spectra.

### ZnMgAl coatings

The ZnMgAl coating for this study was prepared at the production line of voestalpine Stahl GmbH by hot-dip galvanizing of cold rolled steel sheets. The coating layers exhibit a thickness of about 8  $\mu\text{m}$ , adjusted by air knives immediately after the dipping bath, which consists of an

alloy with 96 wt% Zn, 2 wt% Mg, and 2 wt% Al. Furthermore, the coating was subsequently subjected to a skin-passing procedure [17].

For the corrosion tests, a flat panel measuring 150×100-mm cut out from the industrially produced coil was used. The panel for the corrosion test was cleaned by means of alkaline solution (Ridoline C72W) and then exposed to the standardized salt spray test (SST) according to DIN EN ISO 9227 (NSS) using 5 wt% of NaCl aqueous solution with pH 7 regulated with NaOH at constant temperature of 35 °C for 8 h.

Prior to the XPS measurement, a sample with dimensions of 20×50 mm was cut out of the corroded panel.

### XPS analysis

For to the measurements, samples were usually mounted on the sample holder using copper clips and the sample holder was electrically grounded during the analysis. In addition, some samples were electrically insulated from the sample holder using microscopic glass slides and the sample holder was not connected to the ground during the measurement in order to examine the role of the sample's grounding to its charging behavior. XPS measurements were performed using a Theta Probe XPS system (ThermoFisher, UK) and assessed by means of the Avantage software package provided by the system manufacturer. Samples were irradiated with the monochromated Al-K $\alpha$  X-Ray source (1,486.6 eV) with a spot size of 400  $\mu$ m and power of 100 W. Spectra were recorded in standard lens mode with pass energy of 50 eV, dwell time of 50 ms, and 20 scans. A pass energy of 50 eV has been chosen as a compromise value, providing for our system a satisfactory energy resolution as well as reasonably high sensitivity/ transmission. Charging effects were compensated by the standard flood gun (FG) charge neutralization device of the XPS system (Dual flood gun FG02, ThermoFisher, UK) delivering simultaneously a beam of low energy electrons (−2 eV) and a beam of low-energy argon ions. Prior to each experiment, the effectiveness of the neutralization was tested and the flood gun parameters were accordingly optimized. The C1s peak of adventitious carbon at 285.0 eV was taken as a reference of charge-shift correction for the measured spectra, including reference spectra. In order to resolve the exact chemistry of corrosion products, a linear combination fitting method included in the Avantage software package was used, which enables the

measured spectra to be reconstructed with chosen reference spectra, recorded by us under the same experimental conditions. The quantitative analysis was performed using the Zn2p<sub>3/2</sub>, O1s, C1s, Cl2p, Mg2p, and Al2p photoelectron lines with linear or Shirley background subtraction and normalization using Scofield sensitivity factors.

## Results and discussion

### Analysis of model mixtures

To verify the chosen strategy for the experimental data evaluation, pure reference chemicals as well as their model mixtures were at first measured with the same experimental parameters. Recorded spectra of pure references—charge shift corrected with respect to the C1s peak—were then further used for the curve fitting of the mixed samples by means of the linear combination method. The determined binding energies of the Zn2p<sub>3/2</sub> peak, kinetic energies of the Zn L<sub>3</sub>M<sub>45</sub>M<sub>45</sub> Auger peak and the calculated modified Auger parameter of the three main reference components ZnO, hydrozincite, and simonkolleite are listed in Table 1.

In Fig. 1 XPS spectra of carbon, oxygen, chlorine, and zinc (Fig. 1a–e) and a Wagner chemical state plot of zinc (Fig. 1f) of a model mixture of hydrozincite and ZnO are at first shown. The spectra (Fig. 1a–e) were here interpreted using the strategy that the measured and charge corrected data is directly fitted with a linear combination of the charge corrected spectra of the pure reference chemicals, hydrozincite, and ZnO. Already the carbon C1s peak of inorganic carbon found at 289.5 eV (Fig. 1a) shows no satisfactory match with the reference peak of the carbonate group from the hydrozincite reference. The oxygen spectrum (Fig. 1b) also cannot be fitted in a satisfactory way as a combination of oxygen peaks from both, hydrozincite and ZnO, with the fitted envelope not matching at all the raw data. Since there is no chlorine-based component present in the analyzed mixture, the chlorine scan (Fig. 1c) exhibits only background noise. Zinc scans of Zn2p<sub>3/2</sub> and ZnL<sub>3</sub>M<sub>45</sub>M<sub>45</sub> peaks fitted with both references reveal contradicting compositions of the mixture: while the standard fitting procedure of the Zn2p<sub>3/2</sub> peak shows ZnO as the main and hydrozincite as minor component of the mixture, the second zinc peak of ZnL<sub>3</sub>M<sub>45</sub>M<sub>45</sub> reveals in contrast hydrozincite as the main component and ZnO as the minor

**Table 1** Binding energy of Zn2p<sub>3/2</sub>, kinetic energy of ZnL<sub>3</sub>M<sub>45</sub>M<sub>45</sub> peaks and modified Auger parameter of measured reference materials: ZnO, hydrozincite, and simonkolleite

Material	BE of Zn2p <sub>3</sub> (eV)	KE of Zn L <sub>3</sub> M <sub>45</sub> M <sub>45</sub> (eV)	MAP (eV)
ZnO	1,021.6	988.3	2,009.9
Hydrozincite	1,021.5	987.8	2,009.3
Simonkolleite	1,021.8	987.5	2,009.3

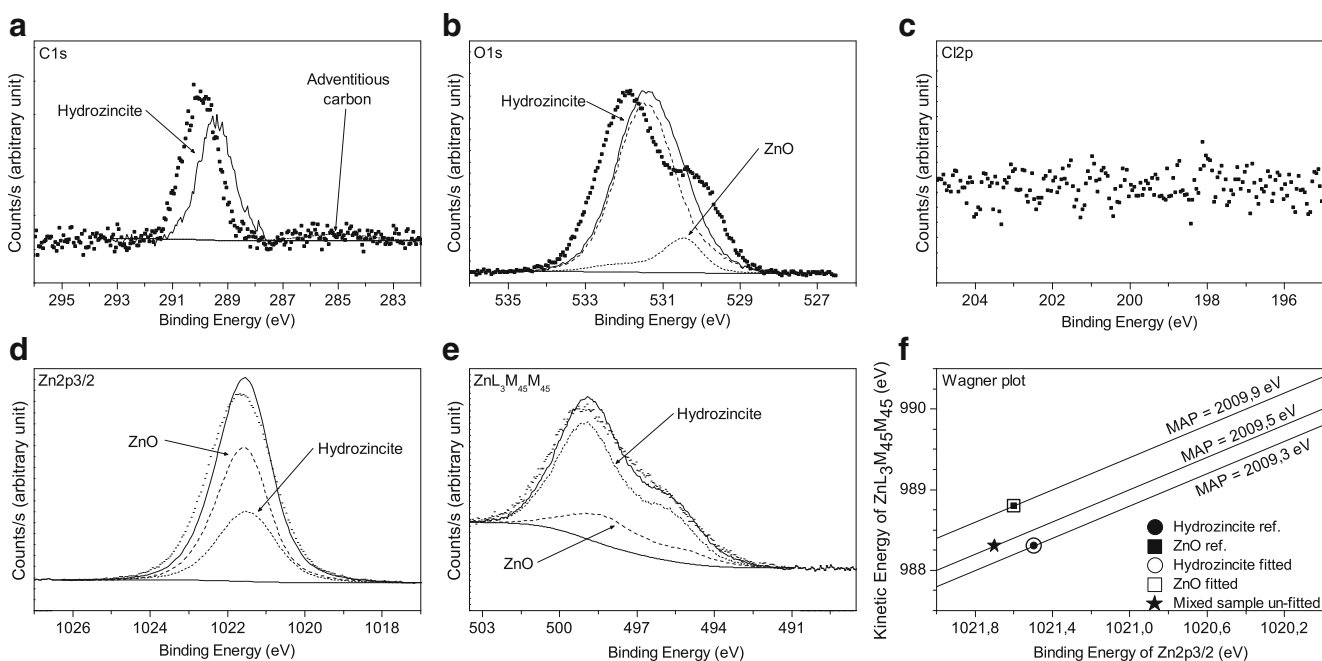


**Fig. 1** XPS peaks of: **a** carbon; **b** oxygen; **c** chlorine; **d**, **e** zinc; and **f** Wagner chemical state plot of a hydrozincite–ZnO mixture of powders fitted by a linear combination fitting method with hydrozincite and ZnO reference spectra

one. The Wagner chemical state plot of Zn (Fig. 1f) shows two facts: (1) the binding, respectively kinetic, energies of the fitted Zn peaks of reference materials are constant, which is in agreement with this fitting strategy, and (2) the point representing the un-fitted Zn peak positions of the mixture possesses a value of the modified Auger parameter (MAP) of

2,009.5 eV, which is between the MAP of hydrozincite (2,009.3 eV) and ZnO (2,009.9 eV), but shifted to higher binding energy (BE) of Zn<sub>2p<sub>3/2</sub></sub> relative to the positions of both references. In total, the performed evaluation of the data using the described standard procedure provides no reasonable result and the known presence of hydrozincite and ZnO

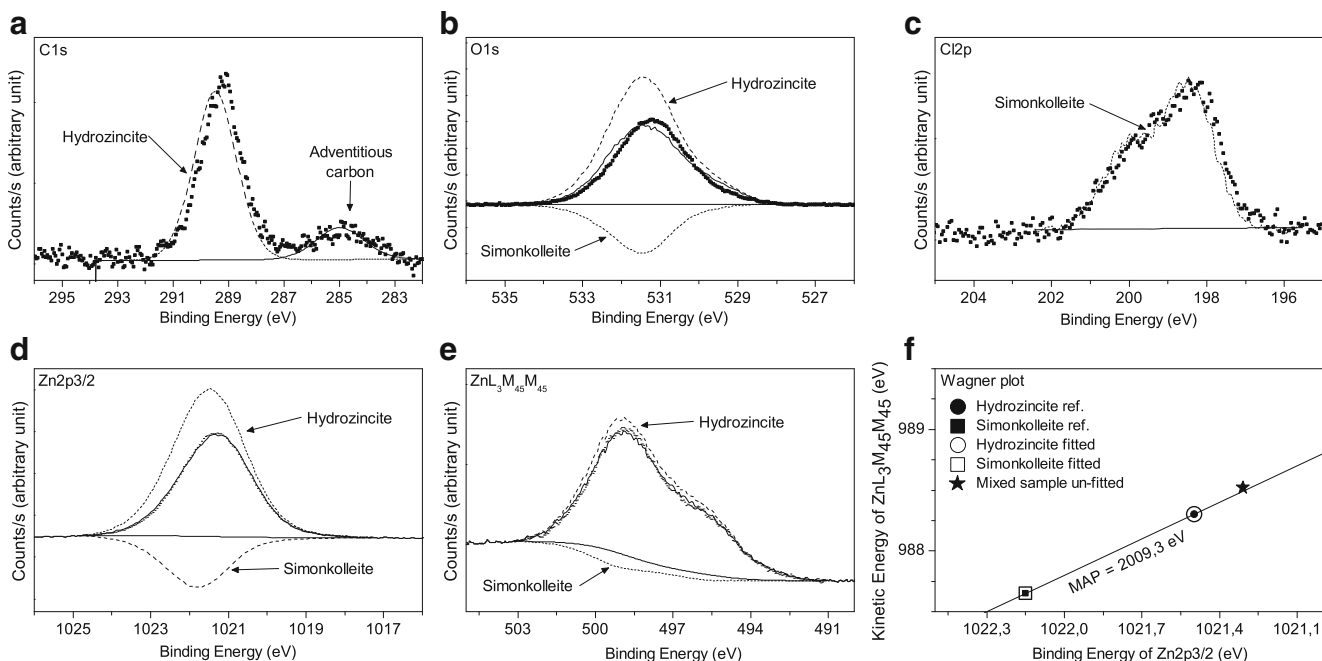


**Fig. 2** XPS peaks of: **a** carbon; **b** oxygen; **c** chlorine; **d**, **e** zinc; and **f** Wagner chemical state plot of a hydrozincite–simonkolleite mixture of powders fitted by a linear combination fitting method with hydrozincite and simonkolleite reference spectra

in the mixed sample could not be proven and reconstructed in a unique way. It is equally evident that the basic and usually taken approach of fitting symmetric peaks into the raw spectra and evaluating the binding energies would also give incorrect results.

The results for the above-presented standard fitting strategy are presented in Fig. 2 for another mixed sample containing hydrozincite and simonkolleite. A very similar behavior is also observed as in the previous case. The fitted carbonate peak of hydrozincite (Fig. 2a) as well as the chlorine peak of simonkolleite (Fig. 2c) does not fully match the raw data of the mixed sample. The oxygen peak (Fig. 2b) and both zinc peaks (Fig. 2d, e) were also unable to be correctly resolved with the reference spectra, since the standard fitting method using a linear combination gives in this case completely incorrect results, represented here as even negative contributions of simonkolleite for demonstration purposes. It is evident that the physical meaningful solution (i.e., negative component is set to zero) has an even higher deviation from the measured spectra, or—if using symmetrically shaped peaks and no reference spectra for fitting—infinately many solutions would be obtained. The Wagner chemical state plot exhibits a similar trend as previously observed, with the position of the un-fitted mixed sample being not in between the positions of both references. Also in this case, the known composition of the mixed sample could not successfully be confirmed by using a linear combination of pure reference spectra.

Despite the fact that the used standard fitting strategy did not work properly to identify the known components of the mixed model samples, a similar trend can be found in both analysis results. Although all measured data was charge corrected via

the  $C_{C-C}$  peak at 285.0 eV prior to the evaluation process, small differences in binding energy between peaks of reference materials and mixed samples can be observed. Whereas such a charge referencing is naturally less precise for minor amounts of adventitious carbon, like in the situation depicted in Fig. 1, this effect is mostly noticeable in Fig. 2a with a pronounced  $C_{C-C}$  peak, and where the fitted carbonate peak of the hydrozincite reference clearly seems to be shifted by 0.4 eV from the peak in the mixed sample, or in Fig. 2c, where similarly the chlorine peak of the simonkolleite reference exhibits a shift of 0.35 eV from the chlorine peak in the mixed sample. The same effect is apparent in both Wagner plots in Figs. 1f and 2f for the zinc peaks.

In order to gain more information for the origin of the above-stated problem with fitting of the model mixed samples, an additional set of measurements of the first samples' system (hydrozincite, ZnO, and hydrozincite–ZnO mixture) was performed by using different ways of sample mounting: (A) all three samples were measured as before, powders were pressed onto the indium foil and conductively mounted on the grounded sample holder; (B, C) samples on indium foil were insulated from the sample holder using a microscopic glass slide; (C) samples were mounted by the same way described as (B), but a lower energy of the flood gun electrons was used (0.5 eV); and (D) all three powder materials were mounted on glass slides using non-conductive double-sided adhesive tape. The results shown in Table 2 reveal again the same problems as demonstrated above by curve fitting: charge shift referencing via adventitious carbon completely failed, since instead of a one certain value of the BE for each peak and each compound/sample a range of BEs was obtained as demonstrated for the  $Zn2p_{3/2}$  peak.

**Table 2** Dependency of measured binding energies of  $Zn2p_{3/2}$  peak on different experimental conditions: electrical insulation of the sample from the sample holder and energy of the flood gun electrons used for charge neutralization

Sample	Measurement condition	$Zn2p_{3/2}$ BE (eV)		
		As measured	Charge corrected	FWHM
ZnO	A	1,021.3	1,021.1	1.4
	B	1,019.1	1,021.2	1.5
	C	1,020.6	1,021.4	1.5
	D	1,019.1	1,021.0	1.4
HZ	A	1,019.7	1,021.7	1.8
	B	1,020.9	1,022.0	1.9
	C	1,022.0	1,022.0	2.0
	D	1,020.0	1,021.3	2.0
ZnO–HZ mixed sample	A	1,020.2	1,021.7	2.0
	B	1,019.7	1,021.2	2.0
	C	1,022.2	1,022.5	2.2
	D	1,019.9	1,021.5	2.0

*A* grounded in foil with pressed powder on top, energy of 2 eV for FG electrons, *B* in foil with pressed powder insulated with glass, energy of 2 eV for FG electrons; *C* in foil with pressed powder insulated with glass, energy of 0.5 eV for FG electrons; *D* powder held on glass, energy of 2 eV for FG electrons

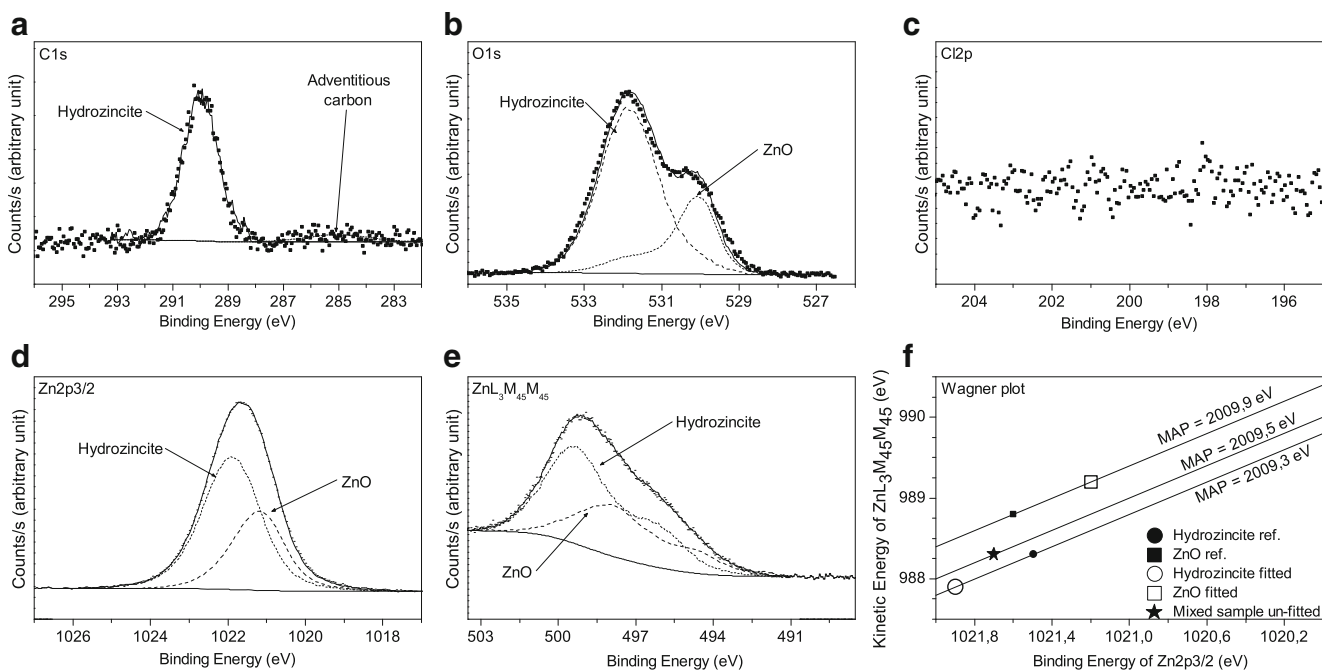


**Fig. 3** XPS peaks of: **a** carbon; **b** oxygen; **c** chlorine; **d**, **e** zinc; and **f** Wagner chemical state plot of the hydrozincite–ZnO mixture fitted with enhanced method with hydrozincite and ZnO reference spectra partially shifted by +0.4 eV for hydrozincite and –0.4 eV for ZnO

A mismatch of the resulting data obtained for two very similar situations, like (B) and (D), clearly indicates no beneficial effect of the sample's electric insulation during measurement. For these reasons, electrically floating the samples did not bring any improvement and cannot be taken as a solution for the identified problem of spectral shifts.

However, a reasonable explanation of the observed phenomenon can be drawn with respect to the model of energy levels and potential energy diagrams as exemplified for different situations of charge build-up in the Al–Al<sub>2</sub>O<sub>3</sub> system proposed in the work of Baer et al. [18]. The stated model shows that if the materials in the measured system are conducting, the Fermi levels of the materials are aligned as well as the potential in the system is constant and all binding energies may be then referenced to the BE of a known component of the system, such as, e.g., the C1s peak of adventitious carbon at 285.0 eV. Furthermore, the efficiency of the charge compensation is known to be affected by many factors, as specimen composition, sample homogeneity, surface conductivity, and surface topography. In addition, the used materials, taken as the simulated products of corrosion, exhibit very different electrical properties (hydrozincite and simonkolleite are known to be insulators [6, 7], on the other hand ZnO is a semiconductor [19]), and the samples' homogeneity cannot be considered to be ideal due to different particle size of the used materials. Thus, the observed differences in binding energies of peaks are attributed to a combination of the misalignment of energy levels among the materials in the samples and formation of steps in the potential or electric fields as well as

unsatisfactory neutralized charge built-up on the samples' surfaces, even though the charge neutralization system was optimized for each sample separately prior to each measurement. Two possible ways were considered in order to solve the above mentioned problem: (1) improvement of the preparation steps of the mixed model samples, e.g., longer milling could result in a more uniform surface composition, and (2) modification of the fitting strategy. Due the heterogeneous nature of corroded ZnMgAl coatings, being in the scope of the second part of this study and with their surface being non-uniform and rough, the second way was chosen for the following work.

#### Enhanced evaluation strategy

As demonstrated above, the original state-of-the-art strategy for XPS data evaluation was found to be inapplicable for complex systems like ZnMgAl corrosion products, so a new evaluation strategy was developed. Taking the observed finding from the previous section into account, differences in the BEs between reference peaks and peaks in model mixtures are considered to be persisting differential charging artifacts and newly, so labeled, peak shift corrections for the reference material spectra were additionally implemented to the evaluation process. These corrections are not constant, but have to be determined for each measurement position, since the environment and charging situation can critically differ. In detail, each evaluated mixed sample was treated separately but in similar fashion, i.e., the peak shift corrections for the spectra of

**Table 3** Comparison of three different fitting approaches using the data acquired at different conditions: as measured (data without any correction, e.g., charge shift correction), fitting with charge shift correction

data (via the adventitious carbon C1s peak at 285.0 eV) and fitting via the proposed advanced method

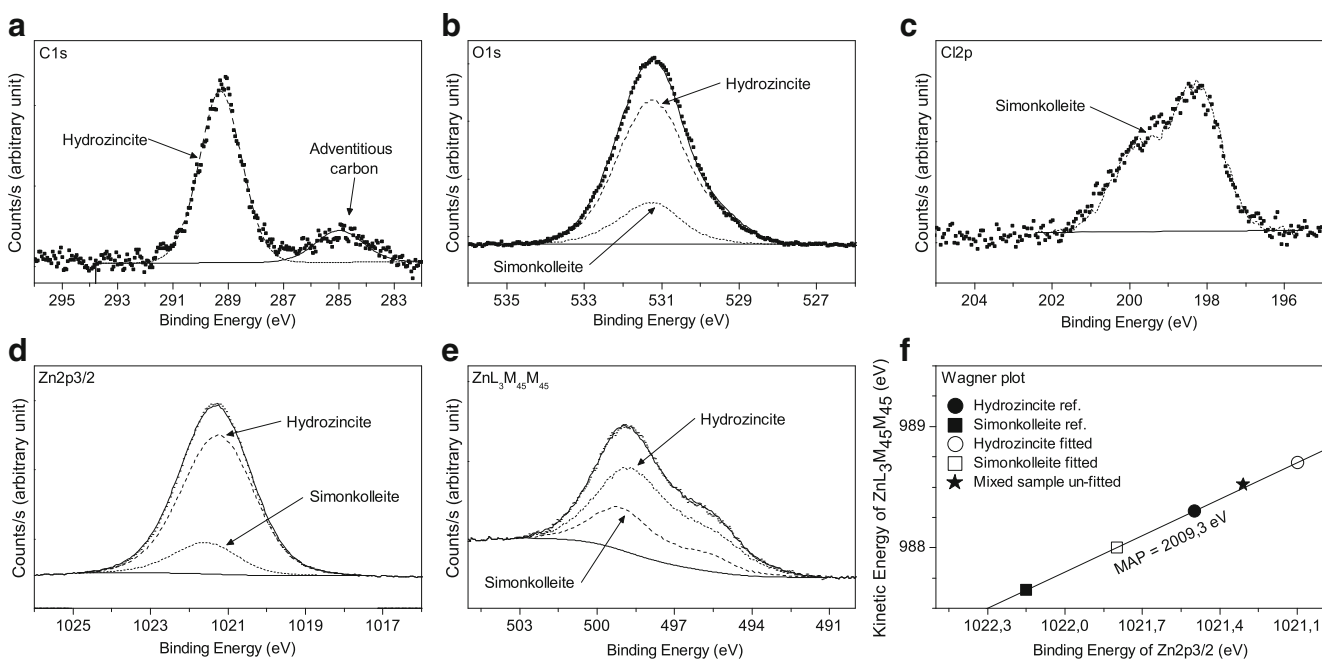
Measurement conditions			Fitting results		
ZnO	HZ	ZnO–HZ mixture	As measured	Charge shift correction	Proposed procedure
A	A	A	✗	✗	✓
B	B	B	✓	✗	✓
C	C	C	✗	✗	✓
D	D	D	✓	✗	✓
D	D	B	✓	✗	✓
A	A	B	✗	✗	✓
B	B	D	✓	✗	✓
A	A	D	✗	✓	✓
B	B	A	✗	✓	✓
D	D	A	✗	✗	✓

✗ failed, ✓ passed

*A* grounded in foil with pressed powder on top, energy of 2 eV for FG electrons, *B* in foil with pressed powder insulated with glass, energy of 2 eV for FG electrons; *C* in foil with pressed powder insulated with glass, energy of 0.5 eV for FG electrons; *D* powder held on glass, energy of 2 eV for FG electrons

reference materials were derived and calculated by following way for each measurement: the BE of a unique selected peak of reference material referenced with respect to adventitious carbon method was subtracted from the normalized BE of the analogous peak of the mixed sample. For instance, the carbonate peak has been chosen for the calculation of the peak shift correction for hydrozincite, since no other used reference

materials contained a carbonate group. For the same reason, the Cl2p peak was used for the determination of the peak shift correction of simonkolleite. Derived values were further applied to shift the remaining peaks of each reference material as O1s, Zn2p, ZnL<sub>3</sub>M<sub>45</sub>M<sub>45</sub>, and the evaluation was then continued by the same way by using fitting with the linear combination method.

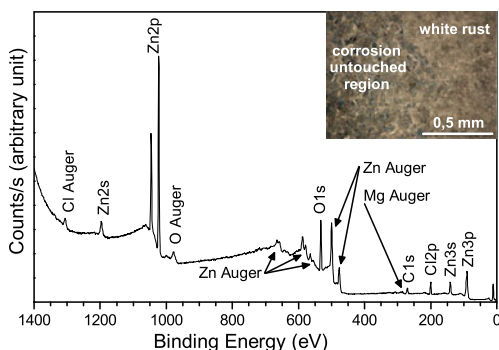
**Fig. 4** XPS peaks of: **a** carbon; **b** oxygen; **c** chlorine; **d**, **e** zinc; and **f** Wagner chemical state plot of the hydrozincite–simonkolleite mixture fitted with enhanced method with hydrozincite andsimonkolleite reference spectra partially shifted by  $-0.4$  eV for hydrozincite and  $-0.35$  eV for simonkolleite

**Table 4** Measured elemental compositions of model mixtures of hydrozincite (HZ)–ZnO and hydrozincite–simonkolleite (Sim)

Peak	Concentration (at. %)	
	HZ–ZnO mixture	HZ–Sim mixture
C <sub>C-C</sub>	0.6	2.0
C <sub>carbonate</sub>	6.4	8.0
Cl	0.0	3.5
Zn	39.9	31.8
O	53.1	54.7

The shift for ZnO in the hydrozincite–ZnO mixture was derived in a two-steps procedure, at first a correction for hydrozincite was calculated using the carbonate peak and applied for the rest of the hydrozincite peaks (O1s, Zn2p, Zn Auger peak), secondly the shift for ZnO was derived by using the O1s peak of the mixed sample, with the already fitted hydrozincite O1s spectrum in it in order to obtain the best match of the fitting envelope with the raw data.

The experimental data of the model mixtures shown in the previous section were now re-evaluated by the suggested modified fitting strategy. In Fig. 3, the re-evaluated analysis of the hydrozincite–ZnO mixture is shown. The calculated peak shift correction of +0.4 eV was applied for the fitted hydrozincite reference spectra, while the ZnO reference peaks were shifted by a value of –0.4 eV, leading to a good match between the fitting envelope and the raw data in all evaluated scans. The effect of the applied peak shift correction is better apparent in the Wagner chemical state plot of Fig. 3f. The application of corrections leaves the values of the modified Auger parameters (MAP) of the fitted references unchanged, in agreement with the claimed independency on physical changes or charging of the sample [20]. MAPs of both fitted hydrozincite and ZnO references kept constant, while their positions in respect to

**Fig. 5** XPS survey spectrum of a ZnMgAl-coated steel sample after a salt spray test, with an optical micrograph of the sample surface in the inset**Table 5** Elemental quantification of detected elements in three points on the white corroded region of a ZnMgAl surface exposed to a SST for 8 h

Peak	Concentration (at.%)		
	Point 1	Point 2	Point 3
C <sub>C-C</sub>	4.1	3.5	5.5
C <sub>carbonate</sub>	8.5	2.9	7.2
Cl	0.9	11.0	3.7
Zn	30.6	39.1	28.3
O	52.7	42.9	50.4
Mg	2.2	0.0	3.7
Al	0.5	0.6	0.5
Na	0.6	0.0	0.7

both axes are shifted by the amounts of the calculated peak shift corrections. Newly, the point of the un-fitted mixed sample is situated in between both reference components.

In addition, the effectiveness of the newly discussed method was proven by using the experimental data for the system hydrozincite–ZnO, measured under different mounting and neutralizing conditions, as introduced in Table 2, with a measurement uncertainty between  $\pm 0.1$  and  $\pm 0.2$  eV. The data were now evaluated in different ways, at first by linear combination peak fitting using the raw data of reference and mixture without any charge corrections (as measured), by means of the first introduced standard fitting method with charge referencing to adventitious carbon and finally by means of the newly discussed method with additional peak shift corrections. The result of this comparative evaluation is shown in Table 3, revealing that the standard method very often failed, even though in a few situations it provided a reasonably good result. However, using no charge referencing at all leads in even more cases to success. In contrast, the newly developed and discussed method provided always good results, independently on the measurement conditions of reference and mixture samples. In other words the presented method demonstrated its ability to bring correct results for any situation. This is especially important for corrosion products which may experience different (and unknown) conductive and non-conductive environments.

Subsequently, the data of the second model mixture of hydrozincite–simonkolleite were re-evaluated by using the same novel procedure. Shift corrections of –0.4 eV for hydrozincite derived by using the carbonate peak and –0.35 eV for simonkolleite by using the chlorine Cl2p level were applied, with the results shown in Fig. 4. Again a qualitatively good fit was obtained and in contrast to the result of the original fitting shown in Fig. 2, the known components of the model mixture



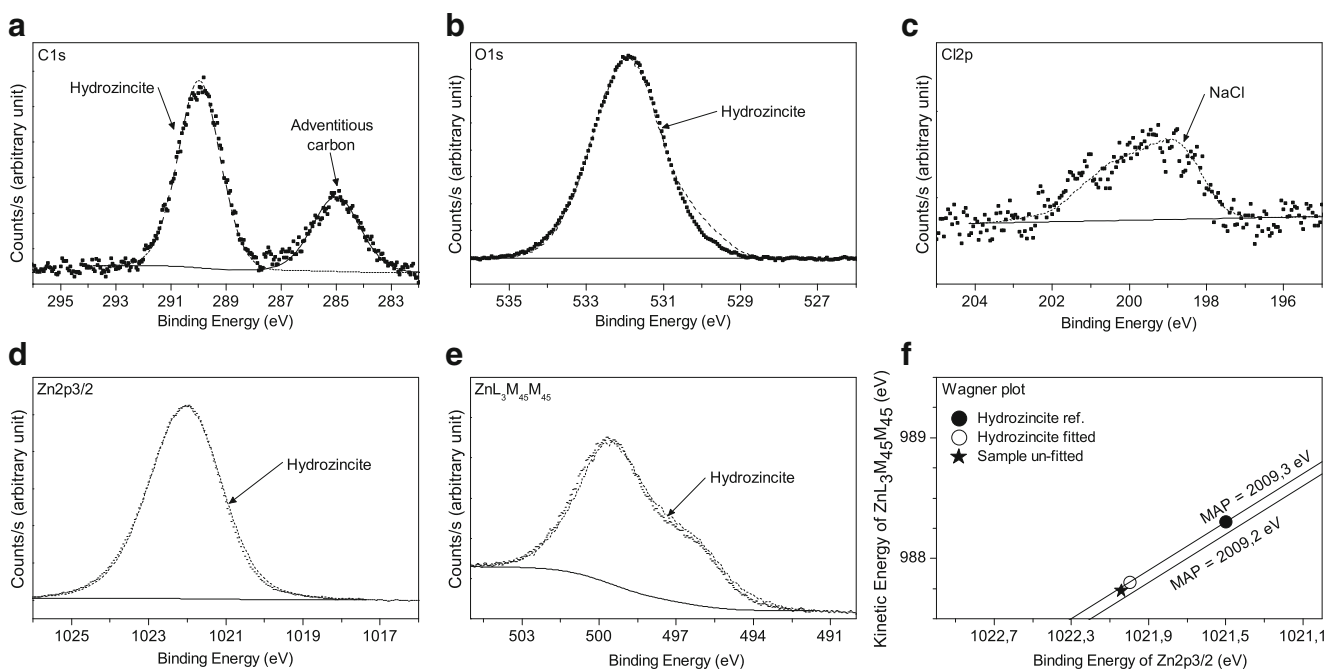


**Fig. 6** XPS peaks of: **a** carbon; **b** oxygen; **c** chlorine; **d**, **e** zinc; and **f** Wagner chemical state plot of one region of the corroded ZnMgAl surface. The peaks were fitted using the proposed advanced method with spectra from the own reference spectra library and interpreted as hydrozincite

are confirmed by the newly developed evaluation method. The Wagner chemical state plot of Zn (Fig. 4f) again demonstrates the effect of the implemented peak shift corrections so that the BE position of the point representing the un-fitted zinc peaks is positioned in between the fitted

references, proving the presence of both, hydrozincite and simonkolleite in the mixture.

Finally, the convincing good qualitative fitting results obtained by the newly established methodology shown in Figs. 3 and 4 were re-checked with respect to the

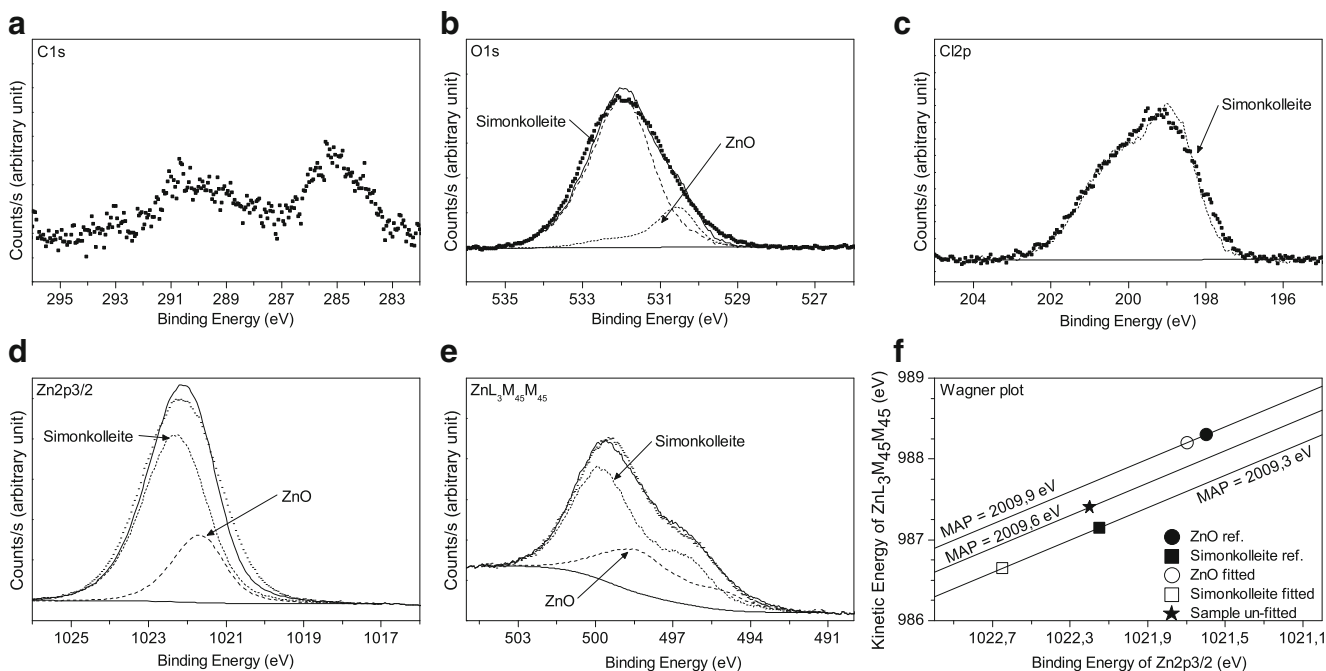


**Fig. 7** XPS peaks of: **a** carbon; **b** oxygen; **c** chlorine; **d**, **e** zinc; and **f** Wagner chemical state plot of a second region of the ZnMgAl-coated steel. The peaks were fitted using the advanced method with reference spectra from the own library and interpreted as a simonkolleite–ZnO mixture

elemental composition of the model samples obtained from their XPS survey and high resolution scans, as presented in Table 4. A good agreement may be found between the ratio of fitted components and concentrations of the elements in both analyzed mixed samples.

#### Analysis of corroded ZnMgAl coatings

The developed evaluation strategy for XPS data as described above, applied and verified on model mixtures of corrosion products, was finally used for the analysis of the industrially produced ZnMgAl coating on steel, corroded in a salt spray test, in order to demonstrate its applicability and reasonability for future corrosion studies and routine analysis of this type of coating. Already by visual inspection, the heterogeneous and rough character of the sample surface is evident as shown in the inset of Fig. 5: the surface of the investigated sample is partially covered with a white layer of assumed corrosion products beside still metallic looking surface regions seemingly unaffected by the corrosion. The white surface layer was subsequently inspected for this study in three spots, with a typical XPS survey spectrum from one measurement position shown in Fig. 5 and exhibiting Zn, C, O, and Cl as main surface constituents.

The detailed chemical analysis performed in the first point on the white surface region revealed an interestingly low content of magnesium (2.2 at.%) and aluminum (0.5 at.%).

The complete results of the elemental quantification are shown in Table 5. Due to the very low concentrations, Mg- and Al-based components were not taken into consideration during the subsequent fitting procedure. In Fig. 6 the evaluated high resolution peaks of (a) carbon, (b) oxygen, (c) chlorine, and (d, e) zinc in that point are shown. The evaluation of the carbon spectrum showed evident presence of mainly inorganic carbon in form of carbonate (BE at 289.9 eV). Adventitious carbon can also be observed, but is not evaluated due to its highly probable origin from contamination of the sample. Since a relatively high concentration of inorganic carbon compared to the other elements is observed, as well as a high concentration of oxygen and zinc, very low concentration of chlorine, the Cs1, O1s, and both Zn peaks were fitted with the hydrozincite reference first. The shift correction of +0.5 eV for the hydrozincite reference was obtained by means of the carbonate peak and applied to all fitted reference spectra. The resulting fit was found to be qualitatively very good. Due to the lack of significant markers for a ZnO reference in form of special groups or elements as, e.g., the carbonate group from hydrozincite or chlorine from simonkolleite, the ZnO reference was tried to be fitted into the already evaluated spectra in order to investigate a possible improvement of fitting. Since the tested reference combination of hydrozincite and ZnO showed worse results than in case of using solely the hydrozincite reference, no significant amounts of ZnO are expected to be

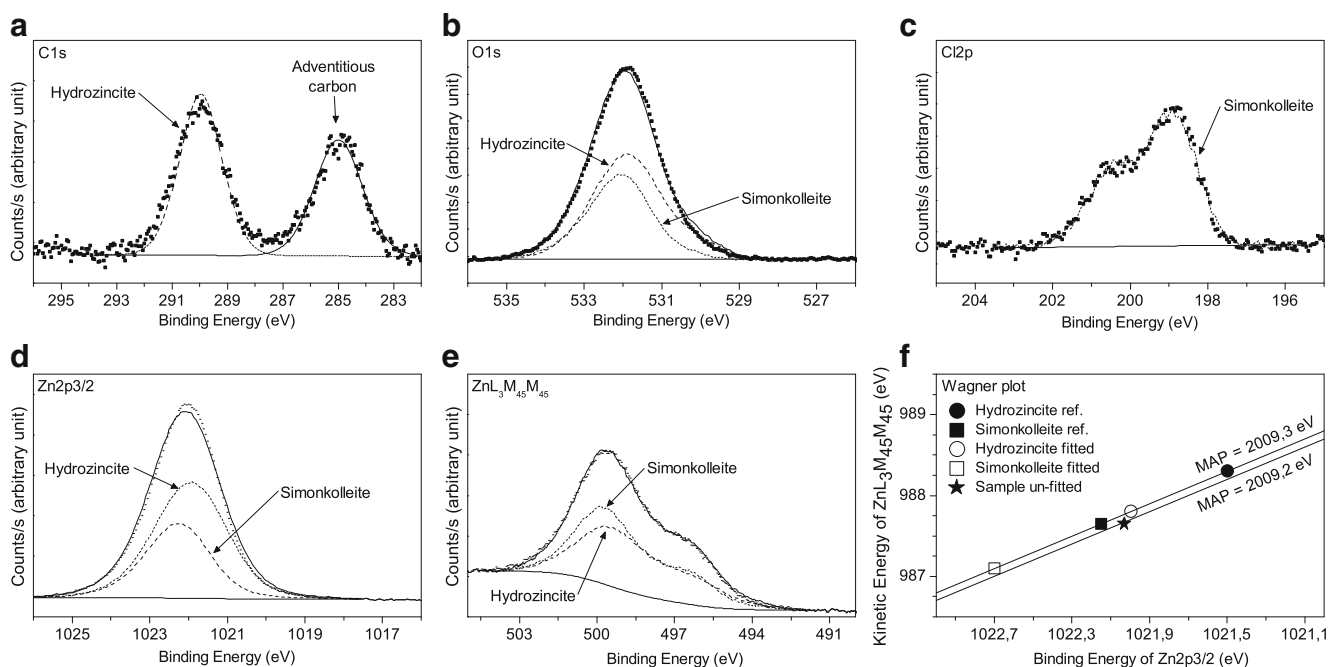


**Fig. 8** XPS peaks of: **a** carbon; **b** oxygen; **c** chlorine; **d, e** zinc; and **f** Wagner chemical state plot of a third region on the corroded ZnMgAl surface, with the peaks again fitted using the enhanced method using

reference spectra from the own spectra library and interpreted as a hydrozincite–simonkolleite mixture

found in the investigated point. The obtained findings are consistent with the Wagner chemical state plot in Fig. 6f: the evaluated value of the MAP of the measured sample is similar to the value of the hydrozincite reference. Chlorine found on the surface in a small amount was linked to the appearance of sodium and fitted as NaCl.

A similar procedure was performed for other two points on the white region of the corroded surface, in their visual appearance being identical to point one. In Fig. 7, the evaluated spectra in the second measurement point are shown. Only traces of Al and no Mg were detected together with a small concentration of C1s carbonate when compared to the previous investigated point, in contrast to chlorine which was found in high concentrations. Due to the slightly asymmetric shape of the oxygen O1s peak, a combination of two references of simonkolleite and ZnO was chosen for the data fitting. Minor deviations of the resulting fit might be explained and caused by the presence of small amounts of hydrozincite. However, regarding the low concentration of the carbonate group, a constituent of hydrozincite, and considering the resulting theoretical amount of Zn originating from hydrozincite, its concentration would be far less than ZnO and even smaller than simonkolleite. For that reason a trial using a combination of three references with simonkolleite, ZnO, and hydrozincite did not result in an improved fit or deliver a more reasonable result. Finally, the Wagner plot in Fig. 7f proves the correctness of the fitting with simonkolleite and ZnO, due to the MAP of the un-fitted original sample (MAP=2,009.6 eV) being in between of the simonkolleite (MAP=2,009.3 eV) and ZnO reference (MAP=2,009.9 eV).

In Fig. 8, the evaluated data finally obtained from a third measured point is shown. Elemental quantification revealed again very low concentrations of aluminum and magnesium. The C1s and C12p scans indicate the presence of both carbonate and chlorine-based corrosion products of zinc. Compared to the first measured point the concentration of carbonate is lower, while the concentration of chlorine is significantly higher. For that reason, references of hydrozincite and simonkolleite were used for the fitting. Prior to the fitting of the oxygen and zinc spectra, shift corrections for both references were calculated by the previously described way and were found to be +0.5 eV for hydrozincite and +0.45 eV for simonkolleite, resulting in qualitatively good fits of all spectra. The Wagner plot in Fig. 8f shows that the un-fitted original value of MAP (2,009.2 eV) is close to the value of MAP =2,009.3 eV for both hydrozincite and simonkolleite references; however, the position of the point of un-fitted sample stands closer to the corrected position of the hydrozincite reference. This coincides with the fact that the major part of the total zinc is bound in hydrozincite and a minor one in simonkolleite.

## Conclusions

In this work, an advanced approach for XPS data evaluation specially dedicated to the chemical assessment of corrosion products formed on the surface of ZnMgAl coatings during corrosion tests was developed and discussed. The importance of the new evaluation strategy for the investigated chemical system was clearly demonstrated at first on model mixtures of pure chemical compounds simulating the assumed chemistry of corroded, heterogeneous surfaces. The usually applied evaluation method, i.e., in general, attributing the chemical states of elements regarding to the value of BEs of peaks and even though enhanced by the application of real shapes/asymmetries of peaks (use of the own reference spectra library), was found to be inappropriate for the investigated system, due to problematic differential charge shifts in the individual spectra which renders routinely applied referencing to the C1s peak of adventitious carbon totally unusable. To cope with the complicated charging–discharging nature of the corrosion products, being in the focus of this work, experimentally derived peak shift corrections were additionally implemented to the evaluation method in order to compensate the negative effect of persisting charging artifacts. As a result, known constituents of tested model mixtures were successfully confirmed, enabling the new method to be applied for the investigation of corroded industrial coatings, as exemplified in a surface analysis of a sample of hot-dip galvanized ZnMgAl coating corroded by means of SST. The obtained results showed that the white corrosion layer exhibits a non-uniform composition containing dominantly Zn-based compounds, whereas only small amounts of Mg and Al were detected. From the chemical states of detected Zn regions covered by hydrozincite, by a combination of hydrozincite–simonkolleite or by simonkolleite–ZnO were identified.

On the basis of the obtained results, the developed evaluation strategy has the potential for a fast and reasonable quantitative analysis of corroded surfaces of ZnMgAl coatings enabling further complex surface investigations of this system including lateral mapping or depth profiling in the future.

**Acknowledgments** Financial support by the Federal Ministry of Economy, Family and Youth and the National Foundation for Research, Technology and Development is gratefully acknowledged.

## References

1. Nishimura K, Shindo H, Kato K, Morimoto Y (1998) Proceeding Galvatech, Chiba, pp. 437–442
2. Komatsu A, Tsujimura T, Watanabe K, Yamaki N, Andoh A, Kittaka T (1999) Patent EP0905270
3. Hagler J, Angeli G, Ebner D, Luckeneder G, Fleischanderl M, Schatzl M (2008) ProcEurosteel, Graz, pp. 1–6

4. Faderl J, Angeli G, Luckeneder G, Tomandl A (2008) Proc SCT, Wiesbaden, pp. 1–8
5. Dutta M, Halder AK, Singh SB (2010) Surf Coat Technol 205:2578–2584
6. Volovitch P, Allely C, Ogle K (2009) Corros Sci 51:1251–1262
7. Volovitch P, Vu T (2011) N, Allely C, Abdel Aal A, Ogle K. Corros Sci 53:2437–2445
8. Schurz S, Luckeneder GH, Fleischanderl M, Mack P, Gsaller H, Kneissl AC, Mori G (2010) Corros Sci 52:3271–3279
9. Zhang B, Zhou HB, Han EH, Ke W (2009) Electrochim Acta 54:6598–6608
10. Biesinger M, Lau L, Gerson A, Smart R (2010) Appl Surf Sci 257:887–898
11. NIST XPS Database, free online version 3.5, <http://srdata.nist.gov/xps>. Accessed 13 May 2013
12. Moulder J, Stickle W, Sobol P, Bomben K (1995) Handbook of X-ray photoelectron spectroscopy. Physical Electronics, Eden Prairie
13. Hosking NC, Strom MA, Shipway PH, Rudd CD (2007) Corros Sci 49:3669–3695
14. Itani H, Duchoslav J, Arndt M, Steck T, Gerdenitsch J, Faderl J, Preis K, Winkler W, Stifter D (2012) Anal Bioanal Chem 403:663–673
15. Tanaka H, Fujioka A, Futoyu A, Kandori K, Ishikawa T (2007) J Solid State Chem 180:2061–2066
16. Zhao R, Yin C, Zhao H, Liu C (2003) Fuel Process Technol 81:201–209
17. Arndt M, Duchoslav J, Itani H, Hesser G, Riener CK, Angeli G, Preis K, Stifter D, Hingerl K (2012) Anal Bioanal Chem 403:651–661
18. Baer DR, Engelhard MH, Gaspar DJ, Windisch L, Windisch CF (2002) Surf Interface Anal 33:781–790
19. Yi GC, Wang C, Park W (2005) Semicond Sci Technol 20:S22–S34
20. Moretti G (1998) J Electron Spectrosc Relat Phenom 95:95–144